The MMS22L-TONSL Complex Mediates Recovery from Replication Stress and Homologous Recombination

Published in final edited form as:

Mol Cell. 2010 November 24; 40(4): 619–631. doi:10.1016/j.molcel.2010.10.024.

The MMS22L-TONSL complex mediates recovery from replication stress and homologous recombination

Lara O'Donnell[1,*], **Stephanie Panier**[1,2,*], **Jan Wildenhain**[3,*], **Johnny M. Tkach**[4], **Abdallah Al-Hakim**[1], **Marie-Claude Landry**[1], **Cristina Escribano-Diaz**[1], **Rachel K. Szilard**[1], **Jordan T. F. Young**[1,2], **Meagan Munro**[1], **Marella D. Canny**[1], **Nadine K. Kolas**[1], **Wei Zhang**[1,2], **Shane M. Harding**[5], **Jarkko Ylanko**[1], **Megan Mendez**[1], **Michael Mullin**[1], **Thomas Sun**[1], **Bianca Habermann**[6], **Alessandro Datti**[1,7], **Robert G. Bristow**[5], **Anne-Claude Gingras**[1,2], **Michael D. Tyers**[1,2,3], **Grant W. Brown**[4], and **Daniel Durocher**[1,2,§]

[1] Samuel Lunenfeld Research Institute, Mount Sinai Hospital, 600 University Avenue, Toronto, M5G 1X5, Ontario, Canada

[2] Department of Molecular Genetics, University of Toronto, Toronto, Ontario, Canada

[3] School of Biological Sciences, University of Edinburgh, Mayfield Road, Edinburgh EH9 3JR, Scotland, UK

[4] Department of Biochemistry and Donnelly Centre for Cellular and Biomedical Research, University of Toronto, Toronto, ON, Canada M5S 3E1

[5] Radiation Medicine Program, Princess Margaret Hospital-University Health Network and Campbell Family Cancer Research Institute-Ontario Cancer Institute, 610 University Avenue, Toronto, ON, Canada M5G 2M9

[6] Max Planck Institute of Molecular Cell Biology and Genetics, Pfotenhauerstrasse 108, 01307 Dresden, Germany

[7] Department of Experimental Medicine and Biochemical Sciences, University of Perugia, Perugia, Italy

Summary

Genome integrity is jeopardized each time DNA replication forks stall or collapse. Here, we report the identification of a complex composed of MMS22L (C6ORF167) and TONSL (NFKBIL2) that participates in the recovery from replication stress. MMS22L and TONSL are homologous to yeast Mms22 and plant Tonsoku/Brushy1, respectively. MMS22L-TONSL accumulates at regions of ssDNA associated with distressed replication forks or at processed DNA breaks, and its depletion results in high levels of endogenous DNA double-strand breaks caused by an inability to complete DNA synthesis after replication fork collapse. Moreover, cells depleted of MMS22L are highly sensitive to camptothecin, a topoisomerase I poison that impairs DNA replication progression. Finally, MMS22L and TONSL are necessary for the efficient formation of RAD51 foci after DNA damage and their depletion impairs homologous recombination. These results indicate that MMS22L and TONSL are genome caretakers that stimulate the recombination-dependent repair of stalled or collapsed replication forks.

[§]Address correspondence to: Daniel Durocher, Ph.D., Samuel Lunenfeld Research Institute, Mount Sinai Hospital, Room 1073, 600 University Avenue, Toronto, ON, CANADA, Tel: 416-586-4800 ext. 2544, durocher@lunenfeld.ca.

[*]These authors contributed equally to this work

Keywords

DNA double-strand breaks; DNA replication; Homologous recombination; siRNA; RAD51; camptothecin

INTRODUCTION

The DNA replication fork and its associated factors, referred to as the replisome, must overcome DNA lesions and structures that impede fork progression to complete DNA replication (Labib and Hodgson, 2007). Failure to appropriately manage these obstacles results in replisome stalling or demise, which can be associated with the formation of DNA double-strand breaks (DSBs), DNA lesions that are potent inducers of genome rearrangements (Budzowska and Kanaar, 2009). Cells therefore commit considerable effort into the management of replication fork progression as a *sine qua non* for genome integrity.

Many activities help the replisome navigate through the obstacles it encounters during DNA replication. One of the best studied is ATR-dependent signaling, which stabilizes stalled replisomes in a state that is competent for the resumption of DNA replication (Casper et al., 2002; Lopes et al., 2001; Tercero and Diffley, 2001). The ATR kinase is recruited to distressed forks via the recognition of single-stranded (ss)DNA bound to the heterotrimeric replication protein A (RPA) complex. Its importance for the maintenance of genome integrity is illustrated by the observation that deletion of the genes encoding components of the ATR signaling cascade in mice invariably results in lethality associated with chromosome breakage (Cimprich and Cortez, 2008).

RPA-bound ssDNA produced at distressed replication forks represents an important platform for the mobilization of other fork-management activities. For example, TIPIN or the recently described HARP annealing helicase are both able to recognize the RPA32 subunit of RPA to directly promote fork progression (Driscoll and Cimprich, 2009; Unsal-Kacmaz et al., 2007). Another critical fork-management system controlled by RPA associated with ssDNA is homologous recombination (HR), which plays an important role in the repair of replication forks or the repair of daughter strand gaps by post-replicative repair (Budzowska and Kanaar, 2009; Wyman and Kanaar, 2006). The contribution of HR in the promotion of DNA replication is perhaps best illustrated by the observation that sister chromatid exchanges (SCEs) are stimulated by agents that induce replication stress (Ribas et al., 1996). Furthermore, disruption of many HR-coding genes, such as *RAD51*, *BRCA2* and *XRCC2*, causes embryonic lethality in mice, consistent with a key role in DNA replication (Budzowska and Kanaar, 2009).

To uncover modulators of genome integrity, we interrogated an RNA interference (RNAi) screen dataset and identified MMS22L (C6ORF167) as a factor required to prevent abnormally high levels of spontaneous DSBs. MMS22L is related to the yeast Mms22 protein, but unlike its budding yeast counterpart it does not interact with a cullin-based ubiquitin ligase (Mimura et al., 2010; Zaidi et al., 2008). Rather, MMS22L forms a complex with TONSL (also known as NFKBIL2), a previously unrecognized homolog of the plant DNA repair protein Tonsoku/Brushy1/Mgoun3. MMS22L-TONSL physically interacts with components of the replication fork and is recruited to RPA-bound ssDNA to promote the loading of RAD51 during HR. Depletion of MMS22L or TONSL results in a marked hypersensitivity to the topoisomerase I poison camptothecin (CPT), which is most likely caused by an inability to promote RAD51-mediated repair of broken replication forks. Our results suggest that MMS22L-TONSL is a recombination mediator important for the promotion of genome integrity in S-phase.

RESULTS

MMS22L prevents the accumulation of replication-associated DSBs

We carried out an RNAi screen that led to the identification of RNF8 and RNF168 (Kolas et al., 2007; Stewart et al., 2009). The screen was based on the quantitation of 53BP1 accumulation in subnuclear foci following gene knockdown with SMARTpool short interfering (si) RNAs. While we focused initially on genes involved in the focal accumulation of 53BP1 at sites of DNA damage, the screen also identified siRNAs that resulted in increased 53BP1 foci. Since our screen assessed 53BP1 foci 24 h after irradiation (Kolas et al., 2007), the siRNAs leading to elevated numbers of 53BP1 foci could either target a DSB repair gene or a gene that prevents the formation of accidental DNA breaks during the cell cycle. In this study, we sought to mine the screen to uncover genes that affect either of these processes. The primary data from the screen can be found in File S1.

As a first validation step, we tested whether a single siRNA duplex, purchased from a supplier (Qiagen) other than the library supplier (Dharmacon), could be used to confirm screen hits. This secondary assay validated 30 hits, including proteins whose depletion was known to increase levels of DSBs, such as the ribonucleotide reductase subunits RRM1 and RRM2, EMI1 (FBXO5), FLASH (CASP8AP2) and REV3L (Table S1) (Machida and Dutta, 2007;Paulsen et al., 2009;Van Sloun et al., 2002) or those known to participate in DNA repair, such as CtIP (RBBP8). A more comprehensive validation of the hits is still ongoing and will be published elsewhere. Nevertheless, a number of uncharacterized genes were also present in this hit list. In particular, we were drawn to C6ORF167 since it had been found to interact with the histone chaperone ASF1 in an interaction proteomics study (Ewing et al., 2007). BLAST searches with C6ORF167 revealed homology to Mms22, an important but poorly characterized regulator of genome integrity in fungi (Figure S1) (Bennett et al., 2001;Dovey and Russell, 2007;Duro et al., 2008;Yokoyama et al., 2007). This sequence relationship was particularly intriguing since Mms22 has long been considered an orphan genome integrity protein without homologs in mammals and was therefore chosen for further characterization.

To reflect the sequence relationship between Mms22 and C6ORF167, we now refer to C6ORF167 as MMS22-Like (MMS22L). We first generated an antibody that recognizes MMS22L by immunoblotting (Figure 1A) and next tested whether MMS22L depletion caused spontaneous DSBs in the absence of exogenous DNA damage. We examined MMS22L knockdown with 7 siRNA duplexes (3 siGENOME and 4 ON-TARGETplus siRNAs) and found that 5/7 increased 53BP1 foci without the application of any other form of DNA damaging agent (Figure 1BC). Moreover, we found that the extent of 53BP1 foci correlated closely with the extent of protein knockdown (Figure S2A) strongly indicating that MMS22L depletion results in the accumulation of endogenous DSBs.

Since endogenous DSBs are often the consequence of aberrant DNA replication, we tested whether the inhibition of origin firing with a CDC7 kinase inhibitor, PHA767491 (Montagnoli et al., 2008) could mitigate the increase in 53BP1 foci observed upon MMS22L depletion. As a positive control, we also examined the effect of PHA767491 on CHK1 (CHEK1) knockdown, which is known to result in replication-associated DSBs (Syljuasen et al., 2005). As shown in Figures 1D and S2B, we observed that PHA767491 treatment reduced the number of 53BP1 foci-positive cells following MMS22L depletion, and to a similar extent following CHK1 knockdown. This result suggested that the DSBs observed in MMS22L-depleted cells are the consequence of an impaired DNA replication-associated process. Consistent with the accumulation of DNA lesions, MMS22L-depleted cells showed robust accumulation in the G2 phase of the cell cycle, with concomitant phosphorylation of CHK1 on S317, indicative of checkpoint activation (Figure 1E-G). This was also observed

using at least two independent siRNAs (Figure S2CD). From these observations, we conclude that MMS22L promotes genome integrity in S-phase.

MMS22L forms a complex with TONSL/NFKBIL2

To gain insight into the molecular mechanism by which MMS22L prevents DNA breaks during DNA replication, we sought MMS22L-interacting proteins. This effort was also motivated by the observation that fungal Mms22 interacts with Mms1, a DDB1-related protein, and with Rtt101, a CUL4-like cullin (Dovey et al., 2009; Mimura et al., 2010; Zaidi et al., 2008). We engineered a HEK293 cell line that stably expressed MMS22L tagged at the C-terminus with myc and Flag epitopes (MMS22L-mFlag) in order to immunopurify MMS22L complexes for mass spectrometric analysis. Peptides derived from the MCM (MCM2, 4, 6, 7) and FACT (SUPT16H and SSRP1) complexes were found in the MMS22L immunoprecipitates (Figure 2A and Table S2). In addition, we also identified a large number of peptides derived from NFKBIL2 (or IKBR), a protein previously thought to be similar to IκB (Figure 2A and Table S2) (Ray et al., 1995). Strikingly, we did not observe any peptides derived from cullins or DDB1, suggesting that MMS22L forms a complex that has a different architecture than its yeast relative.

Examination of the NFKBIL2 sequence revealed the presence of 3 ankyrin (ANK) repeats that are similar to those found in BARD1, but also 8 tetratricopeptide (TPR), 7 leucine rich (LRR) repeats and a ubiquitin-like domain (UBL) that are not found in IκB (Figure 2B). Strikingly, this domain organization revealed that NFKBIL2 is homologous to a protein found in plants called Tonsoku (Suzuki et al., 2004), Bru1 (Takeda et al., 2004) or Mgoun3 (Guyomarc'h et al., 2004) (Figure S3). This observation was of particular importance given that Tonsoku mutants are hypersensitive to a variety of genotoxins (Takeda et al., 2004) and show hallmarks of constitutive DNA damage (Suzuki et al., 2005; Takeda et al., 2004). To reflect the observation that NFKBIL2 is a sequence relative of Tonsoku rather than IκB, we refer to it hereafter as TONSL (Tonsoku-like).

We next raised an antibody that recognizes endogenous TONSL by immunoblotting (Figure 2C) and used it in co-immunoprecipitation studies. We observed that MMS22L and TONSL efficiently immunoprecipitated one another (Figure 2D), suggesting that MMS22L and TONSL form a complex in vivo.

MMS22L-TONSL interacts with the MCM complex

An N-terminally tagged Flag-TONSL protein, expressed inducibly in HEK293 cells, was subjected to immunopurification followed by mass spectrometric analysis. As expected, we recovered many peptides derived from MMS22L (Figure 2E and Table S2). Also, as observed with MMS22L complexes, we identified peptides derived from the MCM (MCM2, 4, 6, 7) and FACT complexes. Moreover, peptides originating from RPA (RPA1 and RPA3), histone H2A, H2B, as well as the histone chaperone ASF1b were detected.

Co-immunoprecipitation experiments with Flag-TONSL validated the interaction with components of the MCM complex (either MCM2 or multiple MCM proteins using a pan-MCM antibody) and a weaker interaction with ASF1b, which is itself a MCM-interacting protein, (Groth et al., 2007) but not with FACT complex components (Figure 2F and data not shown). Intriguingly, we have so far been unable to detect the TONSL-MCM interaction with a TONSL antibody. As expected, we were able to detect a strong interaction between Flag-tagged MMS22L and GFP-tagged TONSL in reciprocal co-immunoprecipitation experiments (Figures 2F and S4A), further confirming that MMS22L and TONSL form a complex. Interestingly, MCMs and MMS22L interact with two different sites on TONSL. As shown in Figure S4B-D, deletion mapping experiments indicate that the integrity of the

C-terminal LRR repeats is necessary for interaction with MMS22L whereas the N-terminal TPR repeats are essential for the interaction with the MCM complex, with a contribution of the ANK repeats.

Consistent with TONSL being part of a functional complex with MMS22L, we observed that depletion of TONSL by multiple siRNAs in RPE1-hTERT cells resulted in an accumulation of cells in G2/M phase (Figure 3A and S5AB). Furthermore, the G2/M accumulation phenotype was also observed in U2OS cells (Figure S5C) and, importantly, could be totally rescued by reintroduction of a siRNA-resistant TONSL cDNA (Figure S5CD) ruling out the possibility that the phenotype was due to an off-target effect. Depletion of TONSL in HeLa cells resulted in an increase in 53BP1 foci but the extent of this increase was less than that observed following MMS22L knockdown (Figure 3BC). Interestingly, TONSL knockdown in HeLa cells resulted in a decrease in MMS22L protein levels (Figure S5A). MMS22L knockdown in HeLa cells also impacted TONSL protein levels (Figure S2D) but the strength of this interdependency was variable depending on the length of the knockdown or the cell type used (e.g. see Figure S5E). Together, these results suggest that MMS22L and TONSL may be part of an obligatory complex, and that TONSL links the complex to the MCM helicase.

The MMS22L-TONSL complex promotes survival following replication fork collapse

The replication-dependent DSBs caused by depletion of MMS22L and the interaction with the MCM helicase suggest a role for the MMS22L-TONSL complex during DNA replication. Therefore, we tested whether depletion of MMS22L by siRNA renders cells hypersensitive to ionizing radiation (IR) or topoisomerase I inhibition by camptothecin (CPT). We observed a striking hypersensitivity of MMS22L-depleted cells to CPT, but not to IR (Figure 3D). Since CPT results in replication stress that is often associated with fork collapse and attendant DSBs (Pommier, 2006), these results suggested that the MMS22L-TONSL complex is particularly important for dealing with replication fork stalling or collapse. The hypersensitivity to CPT can be partly explained by the observation that MMS22L-depleted cells have a marked delay in completing the cell cycle after release from CPT treatment (Figure 3E). Interestingly, MMS22L-depleted cells initiated DNA synthesis after CPT removal yet clearly experienced difficulties in completing DNA replication since the delay in cell cycle progression was associated with CHK1 activation (Figure 3F). These data indicate that MMS22L promotes recovery from DNA replication stress.

Next, we monitored replication dynamics at the single-molecule level using dynamic molecular combing, in which stretched DNA fibers are deposited on glass slides and analyzed by immunofluorescence detection of incorporated nucleotide analogs such as CldU or IdU (Herrick and Bensimon, 2009). First, we examined whether MMS22L was important for unchallenged DNA synthesis in U2OS cells. Replicons undergoing DNA synthesis were labelled for 30 min with CldU and then for 45 min with IdU (Figure 4A). We then specifically analyzed IdU tracts that emanated from a CldU tract, since this labelling strategy enriched for forks that were active at the beginning of the labelling experiment. This scheme did not reveal any difference in the IdU tract lengths or fork velocities between the control and MMS22L-depleted cells (Figure 4A-C) indicating that MMS22L is not required for bulk DNA replication fork progression.

Next, we examined replication fork dynamics in response to CPT, since MMS22L-depleted cells are particularly sensitive to topoisomerase I inhibition. DNA replication is rapidly slowed in the presence of CPT and new origin firing is inhibited via a CHK1-dependent process (Seiler et al., 2007). Using the experimental scheme depicted in Figure 4D, we found that MMS22L-depleted cells are particularly defective in resuming normal DNA replication after removal of CPT (Figure 4DE). These differences in IdU tract length

distributions were highly significant ($p<0.0001$, Mann-Whitney test). Therefore, MMS22L is important for DNA replication fork progression in the presence of DNA lesions. This molecular defect associated with the loss of MMS22L could account for the hypersensitivity to CPT, the accumulation of cells in G2/M and the spontaneous DNA breaks seen in MMS22L-depleted cells.

MMS22L-TONSL accumulates at DNA damage sites

The phenotypes associated with MMS22L and TONSL depletion suggest that the complex might play a direct role at DNA lesions. To test this possibility, we first examined whether MMS22L and TONSL accumulate at sites of laser microirradiation. We observed a near-perfect accumulation of MMS22L (either epitope-tagged or endogenous protein) and TONSL at sites of DNA damage marked by either RPA (Figure 5AB) or γ-H2AX (Figure S6A-C), the former marker identifies sites of replication-associated DSBs whereas the latter is indicative of ssDNA caused by the processing of collapsed replication forks or by ssDNA gaps. The specificity of the respective stainings was confirmed following siRNA-mediated depletion (Figures 5C and S6). Interestingly, while the MMS22L/TONSL stripes overlapped perfectly with those formed by RPA32, they were contained within the γ-H2AX-marked domain (Figure S6A-C). This type of staining pattern has been noted before (Bekker-Jensen et al., 2006) and suggests that MMS22L and TONSL colocalize with ssDNA formed following DSB processing.

To test this possibility further, we quantitated the percentage of cells with γ-H2AX stripes that contained either MMS22L or TONSL stripes following depletion of CtIP, a protein that plays a key role in DNA end resection (Sartori et al., 2007). We found that transfection of cells with a CtIP siRNA profoundly reduced MMS22L-mFlag and TONSL accumulation at sites of microirradiation, almost as much as TONSL or MMS22L depletion (Figure 5C). We conclude from these observations that TONSL and MMS22L can accumulate at DNA breaks, downstream of DNA end-resection.

We next examined whether TONSL and MMS22L accumulate in subnuclear foci in response to various DNA damaging agents. We observed a robust accumulation of MMS22L-mFlag or endogenous TONSL in foci with CPT treatment, resulting in the clearest and most striking accumulation (Figures 5D, 6A and S7A). Not surprisingly, TONSL foci overlapped with MMS22L-mFlag foci (Figure S6D), consistent with the two proteins forming a complex. The staining for each protein was specific since it was abolished by their respective siRNAs (Figure 5D). Interestingly, we also noted that knockdown of MMS22L abolished the formation of TONSL foci and vice versa, an observation also seen with laser microirradiation (Figure 5CD). Interestingly, in this particular experiment, depletion of MMS22L greatly impaired TONSL focus formation in response to CPT without affecting TONSL steady-state levels, while TONSL depletion affected MMS22L steady-state levels (Figure S5E). These results indicate that MMS22L is either a recruitment factor for TONSL at sites of DNA damage or that the integrity of the complex is necessary for accumulation at distressed replication forks.

We then examined colocalization of MMS22L-TONSL with γ-H2AX and RPA32 after CPT treatment. We observed a strong overlap between MMS22L-TONSL and RPA32 foci (Figure 5E) but observed at best a partial co-localization with γ-H2AX (Figure S6E). Importantly, upon depletion of the CtIP protein, we observed a reduction in both RPA32 and TONSL foci (Figure S6FG). These results support the data obtained with laser microirradiation and suggest a model where RPA-bound ssDNA acts as a signal for the recruitment of MMS22-TONSL to sites of DNA damage.

MMS22L-TONSL promotes homologous recombination

DNA replication forks that expose ssDNA can be the substrates of the HR apparatus, which acts to restore active DNA replication. The co-localization of the MMS22L-TONSL complex with RPA-coated ssDNA suggests that MMS22L and TONSL might be involved in the HR-dependent repair of stalled or broken replication forks. In support of this possibility, we observed that MMS22L and TONSL accumulated in foci in response to CPT, hydroxyurea (HU), methylmethane sulfonate (MMS) and ultraviolet (UV) light (Figures 6A and S7A), which can all produce DNA replication stress and replication-associated ssDNA accumulation.

The first step in HR is the formation of the RAD51 nucleofilament on ssDNA. The formation of RAD51 foci can be used as a surrogate for the assembly of RAD51 filaments, although not all filaments result in RAD51 foci (Raderschall et al., 1999). We examined whether depletion of MMS22L or TONSL affected RAD51 focus formation in response to CPT or IR and found that in the absence of either protein, RAD51 focus formation was severely curtailed (Figure 6BC). We did not observe a decrease in end-resection following MMS22L-TONSL depletion, as measured by RPA32 focus formation (Figures 6D and S7B); in fact, we observed that MMS22L- and TONSL-depleted cells RPA32 foci persisted following the removal of CPT, supporting the possibility that MMSS2L-TONSL promotes RAD51 nucleofilament formation downstream of ssDNA generation (Figures 6D and S7B). Moreover, at the 72 h time point, we observed a large increase in the mean number of foci in the MMS22L- and TONSL-depleted cells, with an average of 93.4 and 24.7 RPA32 foci respectively, compared to an average of 3.8 foci in the control-transfected cells (Figure S7B and data not shown).

BRCA2 is a major recombination mediator in eukaryotes that plays a key role in promoting RAD51 focus formation after DNA damage (Yuan et al., 1999). BRCA2 also localizes at sites of DNA lesions (Chen et al., 1998). We therefore asked whether MMS22L-TONSL promotes RAD51 loading by enabling BRCA2 to localize to DNA damage sites. Strikingly, we observed that BRCA2 focus formation was unaffected following MMSS22L or TONSL depletion (Figure 6EF), suggesting that MMS22L-TONSL does not act through BRCA2 to promote RAD51 loading on chromatin.

Next, we examined whether the MMS22L-TONSL complex promotes HR by examining gene conversion stimulated by the I-SceI meganuclease using a DR-GFP reporter integrated in a HeLa cell line (Pierce et al., 2001). As expected, RAD51 siRNA transfection severely attenuated the formation of GFP-positive cells when compared to control siRNA-transfected cells (96% reduction; Figure 7A). Depletion of MMS22L and TONSL by multiple siRNAs in the HeLa DR-GFP cell line decreased gene conversion by an average of 60% (Figure 7A).

Sister chromatid exchanges (SCEs) are a type of recombination event that are associated with replication stress. Bloom syndrome cells are characterized by a very high level of SCEs (Chaganti et al., 1974). As a complement to the DR-GFP assay, we examined whether MMS22L depletion affected the high levels of SCEs observed in Bloom syndrome cells using the BLM-deficient ($BLM^{-/-}$) cell line PSG13 and an isogenic cell line, PSNF5, which is complemented with the wild type BLM gene (BLM^{+}) (Gaymes et al., 2002). We found that MMS22L depletion resulted in a decrease in SCE frequency in both cells lines, with a marked decrease in the $BLM^{-/-}$line (Figure 7B, $p < 0.0001$ by a Mann-Whitney test). From this result, we conclude that MMS22L is also important for HR that occurs as a consequence of replication fork stalling or collapse.

The above results hinted that MMS22L-TONSL might be important for cell proliferation or viability in the absence of BLM. To test this possibility, we implemented a multicolour

assay in which the *BLM*$^{-/-}$ and *BLM*$^{+}$ cell lines were first stably transduced with lentiviral vectors expressing fluorescent protein reporters (GFP or RFP). Cells from each genotype were mixed at a 1:1 ratio before plating, and then transfected with control, MMS22L or TONSL siRNAs. 96 h post- transfection, the cell ratio was determined by high-content fluorescence microscopy. As shown in Figure 7C, we observed a selective loss of the *BLM*-deficient cells following TONSL or MMS22L knockdown. Importantly, we obtained the same result when the fluorescent reporters were swapped (Figure 7C). Furthermore, an identical result was obtained when cells were manually counted following MMS22L knockdown (data not shown). These results indicate that the loss of both BLM and MMS22L results in a synthetic genetic interaction, consistent with a role for MMS22L in the resumption of DNA replication after fork stalling or collapse. Interestingly, we also found that deletions of the budding yeast MMS22L and BLM homologs, *MMS22* and *SGS1*, displayed synthetic sensitivity to DNA damaging agents (Figure S7C), perhaps pointing to an evolutionary conservation of this genetic interaction.

Finally, we sought to map the domains important for TONSL function. We engineered a U2OS cell line to express various siRNA-resistant TONSL deletion mutants under the control of a tetracycline-inducible promoter and examined RAD51 focus formation as a readout of TONSL function. We expressed untagged TONSL proteins as we found that epitope tagging affected TONSL function. The uninduced TONSL wild type cell line had reduced RAD51 focus formation after IR, as expected, when compared to cells where TONSL expression was induced (Figure 7D). Interestingly, we found that while the ANK repeats were dispensable for RAD51 focus formation, the LRR and (to a lesser degree) the TPR repeats were important for promoting them (Figure 7D). These data indicate that the interaction between MMS22L and TONSL is critical for the formation of the RAD51 nucleofilament and suggest that the interaction with the MCM helicase also contributes to this function of the MMS22L-TONSL complex.

DISCUSSION

This study uncovers a role for the MMS22L-TONSL complex as a regulator of genome integrity in human cells. We have found that MMS22L-TONSL is recruited to regions of ssDNA generated either by end processing or by replication fork stalling or collapse. At those sites the complex promotes the recombination-dependent repair of DNA lesions by stimulating the loading of RAD51 at sites of DNA damage. As expected of a complex promoting RAD51 polymerization on ssDNA, depletion of MMS22L-TONSL impairs gene conversion. However, perhaps surprisingly, BRCA2 localization to DNA lesions was unaffected following MMS22L-TONSL knockdown. Together, this data suggests that the function of MMS22L-TONSL may be to enable RAD51 loading in the context of chromatin. Indeed, the putative orthologs of MMS22L and TONSL, yeast Mms22 and plant Tonsoku, have both been linked to chromatin modification pathways (Collins et al., 2007; Takeda et al., 2004). Another possibility is that MMS22L-TONSL antagonizes activities that inhibit RAD51 loading on DNA. Whatever the exact mechanism by which MMS22L-TONSL promotes HR, the strong association between HR and malignancies (Helleday, 2010) suggest that genetic alterations of the *MMS22L* and *TONSL* genes might be associated with cancer.

Intriguingly, MMS22L-TONSL promotes RAD51 focus formation in response to IR and CPT, yet MMS22L-TONSL-depleted cells are selectively sensitive to CPT. While one possibility for this apparent selective hypersensitivity to DNA replication stress might be that MMS22L-TONSL promotes fork restart via HR, another and not mutually exclusive function for the complex might be to promote strand-exchange reactions at daughter strand gaps behind the replication fork (Lehmann and Fuchs, 2006; Nagaraju and Scully, 2007).

Indeed, MMS22L-TONSL might be especially important for HR in the absence of DNA ends.

On this last point, we speculate that MMS22L-TONSL might represent a complex analogous to the prokaryotic RecF, RecO and RecR (RecFOR) complex. These proteins mediate assembly of RecA (prokaryotic RAD51) filaments on ssDNA to reactivate replisomes or to promote HR behind replication forks (Courcelle et al., 2003; Michel et al., 2007; Morimatsu and Kowalczykowski, 2003). RecFOR is particularly important for replication fork restart in the absence of PriA (Grompone et al., 2004). The analogy between MMS22L-TONSL and RecFOR is particularly intriguing since MMS22L-TONSL localizes almost perfectly with RPA (and by association ssDNA). We note that despite the assumption that replisomes always run off after encountering a CPT-induced lesion, this might not always be the case and thus a significant fraction of replisomes could stall instead of collapsing. A similar situation has been proposed when the bacterial replisome approaches UV lesions or when converging forks reach an interstrand crosslink (Knipscheer et al., 2009; Michel et al., 2007). In the case of UV lesions, bacterial RecFOR employs a RecA-dependent mechanism to provide time for DNA repair and resumption of replication. A similar mechanism would be advantageous in eukaryotes given the absence of a PriA-like replication restart system. We suggest that a RecFOR-like mechanism of replisome re-activation is a particularly attractive function for the MMS22L-TONSL complex.

EXPERIMENTAL PROCEDURES

Cell culture and transfection

All culture media were supplemented with 10% fetal bovine serum (FBS), 100 U/ml penicillin and 100 μg/ml streptomycin. U2OS cells were cultured in McCoy's medium, HeLa, HEK293 and 293T cells were cultured in DMEM, RPE-1 hTERT cells were cultured in DMEM/F12 (1:1). Transfections to generate stable cell lines were carried out using Effectene Transfection Reagent (Qiagen) following the manufacturer's protocol. Transient transfections were performed using either Effectene or PEI (Polyethylenimine; Polysciences). All inducible TONSL expression cell lines were generated using the Flp-In TREx system (Invitrogen) as described (Stewart et al., 2009).

Drug treatments

The CDC7 kinase inhibitor PHA767491 was purchased from Tocris Bioscience (Ellisville MO). MMS, HU and CPT were purchased from Sigma-Aldrich (St Louis MO).

RNA interference

siRNAs employed in this study were either siGENOME SMARTpools or On-Target Plus deconvolved siRNAs from ThermoFisher or were purchased from Qiagen. RNAi transfections were performed using Dharmafect 1 (ThermoFisher) in a forward transfection mode.

Homologous recombination assay

Homologous recombination capacity was assayed essentially as described (Pierce et al., 2001). HeLa cells carrying the DR-GFP reporter were transfected with various siRNAs. 48 h later the cells were either transfected with the I-SceI expression plasmid pCBASce or mock treated and then grown for an additional 48 h prior to analysis. Cells were harvested by trypsinization, washed twice with PBS, resuspended in 1 ml PBS, passed through a 35 μm cell strainer and analyzed by FACS. FACS profiles were generated with FlowJo analysis software (Tree Star Inc., Ashland OR).

Full details of all other experimental procedures are given in Supplemental Information.

Highlights

- Loss of MMS22L or TONSL results in spontaneous DNA double-strand breaks.
- MMS22L forms an interdependent complex with TONSL.
- MMS22L and TONSL accumulate at lesions containing RPA-bound single-stranded DNA.
- MMS22L-TONSL promotes RAD51 nucleofilament formation and homologous recombination.

Supplementary Material

Refer to Web version on PubMed Central for supplementary material.

Acknowledgments

We are grateful to B. Wouters, J. Chen and R. Greenberg for reagents, to J. Wrana for the establishment of the Lunenfeld robotics facility and to J. Rouse, W. Harper and M. Peter for communicating unpublished results. LOD holds a post-doctoral fellowship from the Canadian Breast Cancer Foundation. SP holds a Vanier Canada Graduate Scholarship, JTFY holds a Banting and Best Doctoral Scholarship from the Canadian Institutes of Health Research (CIHR). AAH and SMH are CIHR Strategic Training Fellows in the Excellence in Radiation Research for the 21st Century (EIRR21) Program. RGB is a Canadian Cancer Society (CCS) Scientist. MDT is a Research Professor of the Scottish Universities Life Sciences Alliance and holds a Royal Society Wolfson Research Merit Award. DD is the Thomas Kierans Chair in Mechanisms of Cancer Development and a Canada Research Chair (Tier 2) in Proteomics, Bioinformatics and Functional Genomics. This work was supported by a grant from European Research Council to MDT, CCS grants #020254 (to GWB), #20203 (to ACG) and #17154 (to RGB), and CIHR grant MOP84297 to DD.

References

Bekker-Jensen S, Lukas C, Kitagawa R, Melander F, Kastan MB, Bartek J, Lukas J. Spatial organization of the mammalian genome surveillance machinery in response to DNA strand breaks. J Cell Biol 2006;173:195–206. [PubMed: 16618811]

Ben-Aroya S, Agmon N, Yuen K, Kwok T, McManus K, Kupiec M, Hieter P. Proteasome nuclear activity affects chromosome stability by controlling the turnover of Mms22, a protein important for DNA repair. PLoS Genet 2010;6:e1000852. [PubMed: 20174551]

Bennett CB, Lewis LK, Karthikeyan G, Lobachev KS, Jin YH, Sterling JF, Snipe JR, Resnick MA. Genes required for ionizing radiation resistance in yeast. Nat Genet 2001;29:426–434. [PubMed: 11726929]

Budzowska M, Kanaar R. Mechanisms of dealing with DNA damage-induced replication problems. Cell Biochem Biophys 2009;53:17–31. [PubMed: 19034694]

Casper AM, Nghiem P, Arlt MF, Glover TW. ATR regulates fragile site stability. Cell 2002;111:779–789. [PubMed: 12526805]

Chaganti RS, Schonberg S, German J. A manyfold increase in sister chromatid exchanges in Bloom's syndrome lymphocytes. Proc Natl Acad Sci U S A 1974;71:4508–4512. [PubMed: 4140506]

Chen J, Silver DP, Walpita D, Cantor SB, Gazdar AF, Tomlinson G, Couch FJ, Weber BL, Ashley T, Livingston DM, Scully R. Stable interaction between the products of the BRCA1 and BRCA2 tumor suppressor genes in mitotic and meiotic cells. Mol Cell 1998;2:317–328. [PubMed: 9774970]

Cimprich KA, Cortez D. ATR: an essential regulator of genome integrity. Nat Rev Mol Cell Biol 2008;9:616–627. [PubMed: 18594563]

Collins SR, Miller KM, Maas NL, Roguev A, Fillingham J, Chu CS, Schuldiner M, Gebbia M, Recht J, Shales M, et al. Functional dissection of protein complexes involved in yeast chromosome biology using a genetic interaction map. Nature 2007;446:806–810. [PubMed: 17314980]

Courcelle J, Donaldson JR, Chow KH, Courcelle CT. DNA damage-induced replication fork regression and processing in Escherichia coli. Science 2003;299:1064–1067. [PubMed: 12543983]

Dovey CL, Aslanian A, Sofueva S, Yates JR 3rd, Russell P. Mms1-Mms22 complex protects genome integrity in Schizosaccharomyces pombe. DNA Repair (Amst) 2009;8:1390–1399. [PubMed: 19819763]

Dovey CL, Russell P. Mms22 preserves genomic integrity during DNA replication in Schizosaccharomyces pombe. Genetics 2007;177:47–61. [PubMed: 17660542]

Driscoll R, Cimprich KA. HARPing on about the DNA damage response during replication. Genes Dev 2009;23:2359–2365. [PubMed: 19833762]

Duro E, Vaisica JA, Brown GW, Rouse J. Budding yeast Mms22 and Mms1 regulate homologous recombination induced by replisome blockage. DNA Repair (Amst) 2008;7:811–818. [PubMed: 18321796]

Ewing RM, Chu P, Elisma F, Li H, Taylor P, Climie S, McBroom-Cerajewski L, Robinson MD, O'Connor L, Li M, et al. Large-scale mapping of human protein-protein interactions by mass spectrometry. Mol Syst Biol 2007;3:89. [PubMed: 17353931]

Gaymes TJ, North PS, Brady N, Hickson ID, Mufti GJ, Rassool FV. Increased error-prone non homologous DNA end-joining--a proposed mechanism of chromosomal instability in Bloom's syndrome. Oncogene 2002;21:2525–2533. [PubMed: 11971187]

Grompone G, Sanchez N, Dusko Ehrlich S, Michel B. Requirement for RecFOR-mediated recombination in priA mutant. Mol Microbiol 2004;52:551–562. [PubMed: 15066040]

Groth A, Corpet A, Cook AJ, Roche D, Bartek J, Lukas J, Almouzni G. Regulation of replication fork progression through histone supply and demand. Science 2007;318:1928–1931. [PubMed: 18096807]

Guyomarc'h S, Vernoux T, Traas J, Zhou DX, Delarue M. MGOUN3, an Arabidopsis gene with TetratricoPeptide-Repeat-related motifs, regulates meristem cellular organization. J Exp Bot 2004;55:673–684. [PubMed: 14966212]

Helleday T. Homologous recombination in cancer development, treatment and development of drug resistance. Carcinogenesis 2010;31:955–960. [PubMed: 20351092]

Herrick J, Bensimon A. Introduction to molecular combing: genomics, DNA replication, and cancer. Methods Mol Biol 2009;521:71–101. [PubMed: 19563102]

Knipscheer P, Raschle M, Smogorzewska A, Enoiu M, Ho TV, Scharer OD, Elledge SJ, Walter JC. The Fanconi anemia pathway promotes replication-dependent DNA interstrand cross-link repair. Science 2009;326:1698–1701. [PubMed: 19965384]

Kolas NK, Chapman JR, Nakada S, Ylanko J, Chahwan R, Sweeney FD, Panier S, Mendez M, Wildenhain J, Thomson TM, et al. Orchestration of the DNA-damage response by the RNF8 ubiquitin ligase. Science 2007;318:1637–1640. [PubMed: 18006705]

Labib K, Hodgson B. Replication fork barriers: pausing for a break or stalling for time? EMBO Rep 2007;8:346–353. [PubMed: 17401409]

Lehmann AR, Fuchs RP. Gaps and forks in DNA replication: Rediscovering old models. DNA Repair (Amst) 2006;5:1495–1498. [PubMed: 16956796]

Lopes M, Cotta-Ramusino C, Pellicioli A, Liberi G, Plevani P, Muzi-Falconi M, Newlon CS, Foiani M. The DNA replication checkpoint response stabilizes stalled replication forks. Nature 2001;412:557–561. [PubMed: 11484058]

Machida YJ, Dutta A. The APC/C inhibitor, Emi1, is essential for prevention of rereplication. Genes Dev 2007;21:184–194. [PubMed: 17234884]

Michel B, Boubakri H, Baharoglu Z, LeMasson M, Lestini R. Recombination proteins and rescue of arrested replication forks. DNA Repair (Amst) 2007;6:967–980. [PubMed: 17395553]

Mimura S, Yamaguchi T, Ishii S, Noro E, Katsura T, Obuse C, Kamura T. Cul8/Rtt101 forms a variety of protein complexes that regulate DNA damage response and transcriptional silencing. J Biol Chem. 2010

Montagnoli A, Valsasina B, Croci V, Menichincheri M, Rainoldi S, Marchesi V, Tibolla M, Tenca P, Brotherton D, Albanese C, et al. A Cdc7 kinase inhibitor restricts initiation of DNA replication and has antitumor activity. Nat Chem Biol 2008;4:357–365. [PubMed: 18469809]

Morimatsu K, Kowalczykowski SC. RecFOR proteins load RecA protein onto gapped DNA to accelerate DNA strand exchange: a universal step of recombinational repair. Mol Cell 2003;11:1337–1347. [PubMed: 12769856]

Nagaraju G, Scully R. Minding the gap: the underground functions of BRCA1 and BRCA2 at stalled replication forks. DNA Repair (Amst) 2007;6:1018–1031. [PubMed: 17379580]

Paulsen RD, Soni DV, Wollman R, Hahn AT, Yee MC, Guan A, Hesley JA, Miller SC, Cromwell EF, Solow-Cordero DE, et al. A genome-wide siRNA screen reveals diverse cellular processes and pathways that mediate genome stability. Mol Cell 2009;35:228–239. [PubMed: 19647519]

Pierce AJ, Hu P, Han M, Ellis N, Jasin M. Ku DNA end-binding protein modulates homologous repair of double-strand breaks in mammalian cells. Genes Dev 2001;15:3237–3242. [PubMed: 11751629]

Pommier Y. Topoisomerase I inhibitors: camptothecins and beyond. Nat Rev Cancer 2006;6:789–802. [PubMed: 16990856]

Raderschall E, Golub EI, Haaf T. Nuclear foci of mammalian recombination proteins are located at single-stranded DNA regions formed after DNA damage. Proc Natl Acad Sci U S A 1999;96:1921–1926. [PubMed: 10051570]

Ray P, Zhang DH, Elias JA, Ray A. Cloning of a differentially expressed I kappa B-related protein. J Biol Chem 1995;270:10680–10685. [PubMed: 7738005]

Ribas G, Xamena N, Creus A, Marcos R. Sister-chromatid exchanges (SCE) induction by inhibitors of DNA topoisomerases in cultured human lymphocytes. Mutat Res 1996;368:205–211. [PubMed: 8692226]

Sartori AA, Lukas C, Coates J, Mistrik M, Fu S, Bartek J, Baer R, Lukas J, Jackson SP. Human CtIP promotes DNA end resection. Nature 2007;450:509–514. [PubMed: 17965729]

Seiler JA, Conti C, Syed A, Aladjem MI, Pommier Y. The intra-S-phase checkpoint affects both DNA replication initiation and elongation: single-cell and -DNA fiber analyses. Mol Cell Biol 2007;27:5806–5818. [PubMed: 17515603]

Stewart GS, Panier S, Townsend K, Al-Hakim AK, Kolas NK, Miller ES, Nakada S, Ylanko J, Olivarius S, Mendez M, et al. The RIDDLE syndrome protein mediates a ubiquitin-dependent signaling cascade at sites of DNA damage. Cell 2009;136:420–434. [PubMed: 19203578]

Suzuki T, Inagaki S, Nakajima S, Akashi T, Ohto MA, Kobayashi M, Seki M, Shinozaki K, Kato T, Tabata S, et al. A novel Arabidopsis gene TONSOKU is required for proper cell arrangement in root and shoot apical meristems. Plant J 2004;38:673–684. [PubMed: 15125773]

Suzuki T, Nakajima S, Inagaki S, Hirano-Nakakita M, Matsuoka K, Demura T, Fukuda H, Morikami A, Nakamura K. TONSOKU is expressed in S phase of the cell cycle and its defect delays cell cycle progression in Arabidopsis. Plant Cell Physiol 2005;46:736–742. [PubMed: 15746155]

Syljuasen RG, Sorensen CS, Hansen LT, Fugger K, Lundin C, Johansson F, Helleday T, Sehested M, Lukas J, Bartek J. Inhibition of human Chk1 causes increased initiation of DNA replication, phosphorylation of ATR targets, and DNA breakage. Mol Cell Biol 2005;25:3553–3562. [PubMed: 15831461]

Takeda S, Tadele Z, Hofmann I, Probst AV, Angelis KJ, Kaya H, Araki T, Mengiste T, Mittelsten Scheid O, Shibahara K, et al. BRU1, a novel link between responses to DNA damage and epigenetic gene silencing in Arabidopsis. Genes Dev 2004;18:782–793. [PubMed: 15082530]

Tercero JA, Diffley JF. Regulation of DNA replication fork progression through damaged DNA by the Mec1/Rad53 checkpoint. Nature 2001;412:553–557. [PubMed: 11484057]

Unsal-Kacmaz K, Chastain PD, Qu PP, Minoo P, Cordeiro-Stone M, Sancar A, Kaufmann WK. The human Tim/Tipin complex coordinates an Intra-S checkpoint response to UV that slows replication fork displacement. Mol Cell Biol 2007;27:3131–3142. [PubMed: 17296725]

Van Sloun PP, Varlet I, Sonneveld E, Boei JJ, Romeijn RJ, Eeken JC, De Wind N. Involvement of mouse Rev3 in tolerance of endogenous and exogenous DNA damage. Mol Cell Biol 2002;22:2159–2169. [PubMed: 11884603]

Wyman C, Kanaar R. DNA double-strand break repair: all's well that ends well. Annu Rev Genet 2006;40:363–383. [PubMed: 16895466]

Yokoyama M, Inoue H, Ishii C, Murakami Y. The novel gene mus7(+) is involved in the repair of replication-associated DNA damage in fission yeast. DNA Repair (Amst) 2007;6:770–780. [PubMed: 17307401]

Yuan SS, Lee SY, Chen G, Song M, Tomlinson GE, Lee EY. BRCA2 is required for ionizing radiation-induced assembly of Rad51 complex in vivo. Cancer Res 1999;59:3547–3551. [PubMed: 10446958]

Zaidi IW, Rabut G, Poveda A, Scheel H, Malmstrom J, Ulrich H, Hofmann K, Pasero P, Peter M, Luke B. Rtt101 and Mms1 in budding yeast form a CUL4(DDB1)-like ubiquitin ligase that promotes replication through damaged DNA. EMBO Rep 2008;9:1034–1040. [PubMed: 18704118]

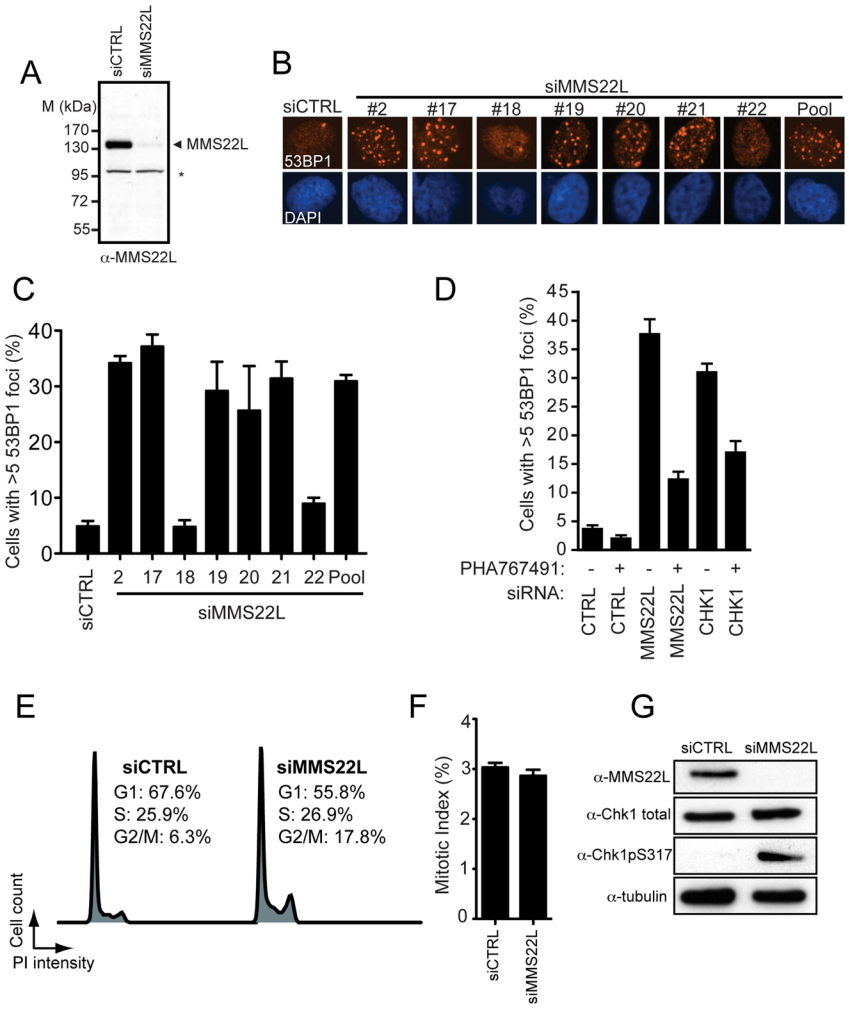

Figure 1. MMS22L prevents spontaneous DNA damage during S phase

(A) Representative immunoblotting of HeLa cells transfected with either control (siCTRL) or MMS22L SMARTpool (siMMS22L). Arrow indicates specific MMS22L band. Asterisk indicates a nonspecific immunoreactive protein that serves as an internal loading control. M, molecular size standards.

(B) Spontaneous 53BP1 focus formation correlates with efficiency of MMS22L knockdown. HeLa cells were transfected with either control or MMS22L siRNAs. 48 h post-transfection cells were fixed and processed for anti-53BP1 immunofluorescence (red) and DAPI staining (blue). An immunoblot documenting the extent of MMS22L depletion is found in Figure S2A.

(C) Quantitation of (B). At least 100 cells per condition were counted. Data are represented as the mean ± SD (n=3).

(D) U2OS cells were transfected either with control, MMS22L or CHK1 siRNAs. 48 h post-transfection, cells were treated either with DMSO or with 5 μM PHA767491 for 6 h, fixed and processed for 53BP1 immunofluorescence. Foci-positive cells were defined as cells with more than 5 53BP1 foci. At least 100 cells per condition were counted. Data are represented as the mean ± SD (n=3).

(E) FACS profiles of hTERT RPE-1 cells transfected with control or MMS22L siRNAs. The proportion of cells in G1, S and G2 phases of the cell cycle are indicated. PI, propidium iodide.

(F) HeLa cells were transfected with either control or MMS22L siRNAs. 48 h post-transfection cells were fixed and processed for anti-phospho-histone H3 immunofluorescence to identify mitotic cells. At least 100 cells per condition were counted. Data are represented as the mean ± SD (n=3).
(G) Depletion of MMS22L results in checkpoint activation. Whole cell extracts of HeLa cells transfected with either control or MMS22L siRNAs were analyzed by immunoblotting with antibodies to CHK1 phosphoserine 317 (pS317), total CHK1 (CHK1), MMS22L or tubulin (loading control).

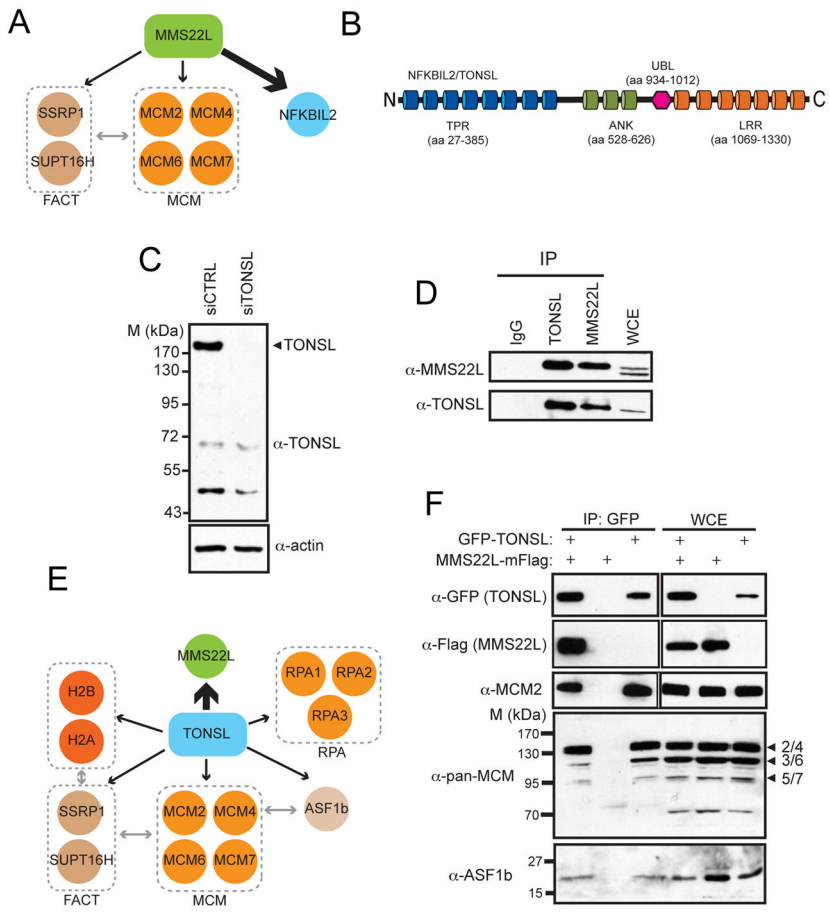

Figure 2. MMS22L interacts with TONSL/NFKBIL2

(A) MMS22L interactions detected by IP-MS (Table S2) grouped according to known biological associations. The strength of interaction is indicated by the boldness of the arrow. Arrows pointing between the different groups indicate a reported biological interaction.

(B) Domain structure of NFKBIL2/TONSL. TPR, tetratricopeptide repeat; ANK, ankyrin repeat; UBL, ubiquitin-like domain; LRR, leucine-rich repeat; aa, amino acid.

(C) Representative immunoblotting of TONSL knockdown. U2OS whole cell extracts were analyzed by immunoblotting with antibodies to TONSL or actin (loading control). Arrow indicates specific TONSL band. M, molecular size standards.

(D) Endogenous MMS22L and TONSL co-immunopreciptiate (IP) each other. A control immunoprecipitation with a non-specific rabbit IgG fraction (IgG) was performed in parallel. Immunoprecipitated proteins were subjected to immunoblot analysis with the indicated antibodies.

(E) TONSL interaction network (Table S2) as described in (A).

(F) Whole cell lysates (WCE) of 293T cells transiently expressing GFP-TONSL and/or MMS22L-mFlag were subjected to immunoprecipitation with anti-GFP antibodies followed by immunoblot analysis with the indicated antibodies. Arrows and numbers at the right indicate the migration of different MCM proteins. M, molecular size standards.

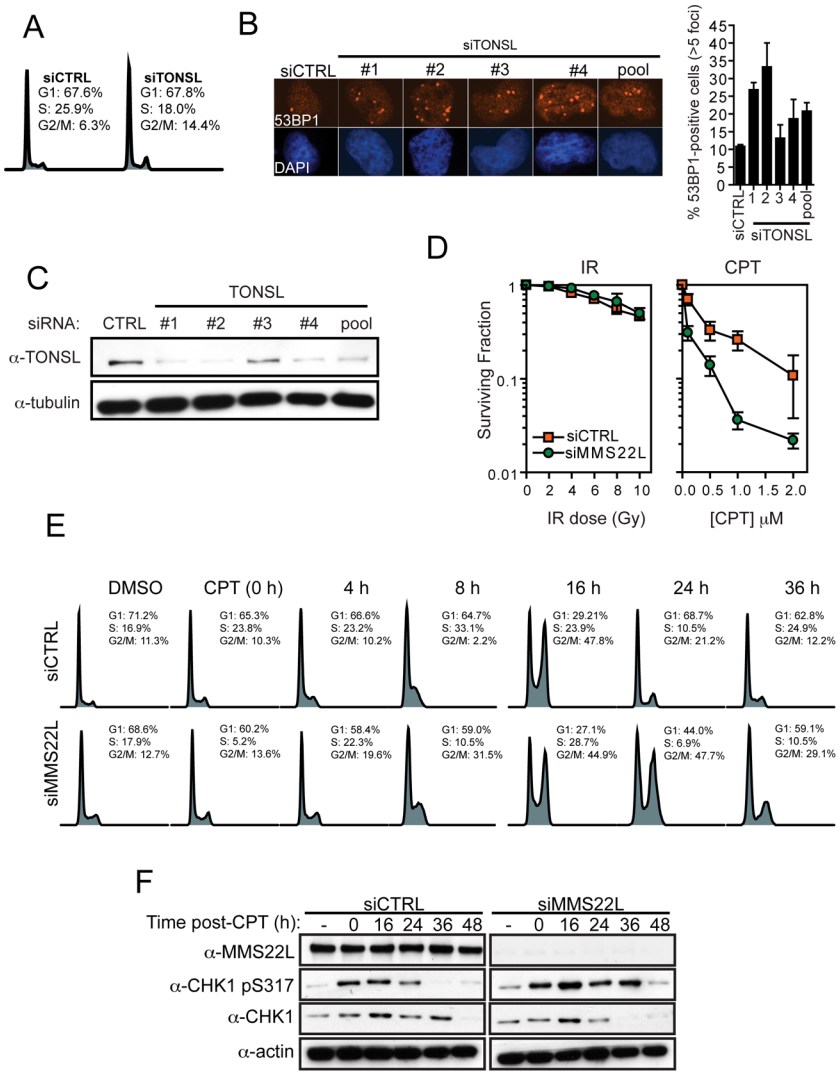

Figure 3. MMS22L and TONSL are required for recovery from replication stress

(A) FACS profiles of RPE-1 hTERT cells 48 h post-transfection with control (siCTRL) or TONSL (siTONSL) siRNAs.

(B) TONSL depletion in HeLa cells results in spontaneous 53BP1 foci. 48 h post-transfection with the indicated siRNAs, cells were fixed and processed for anti-53BP1 immunofluorescence and DAPI staining. Quantitation of 53BP1 foci are shown for each siRNA tested in the accompanying histogram. At least 100 cells per condition were counted. Data are represented as the mean ± SD (n=3).

(C) Immunoblot analysis of transfections shown in (B). Blots of whole cell extracts were probed with antibodies to TONSL and tubulin (loading control).

(D) Clonogenic survival assays in MMS22L-depleted cells following X-irradiation (IR) or treatment with camptothecin (CPT). Cells were then permitted to grow for 14 d before fixation and staining. Colonies with >50 cells were counted. The surviving fraction is represented as the mean ± SD (n=3).

(E) Cell cycle profiles of HeLa cells recovering from a 30 min incubation with 0.1 μM CPT. Cells were transfected with control or MMS22L siRNAs 48 h prior to DMSO or CPT treatment.

(F) HeLa cells were transfected with control or MMS22L siRNAs. 48 h post-transfection, cells were treated with DMSO (-) or 0.1 μM CPT for 30 min and then released into fresh medium for the indicated times. Whole cell extracts were analyzed by immunoblotting with antibodies to MMS22L, CHK1 phosphoserine 317 (pS317), total CHK1 (CHK1) or actin (loading control).

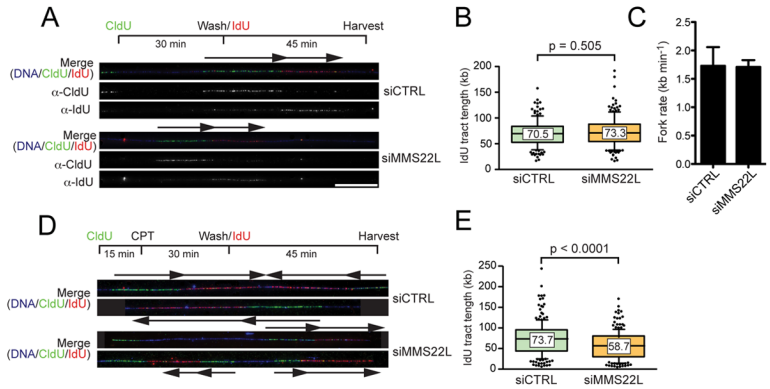

Figure 4. MMS22L promotes DNA replication on damaged templates

(A) Above is a schematic of the fork velocity experiment. Below are representative images of single DNA fibers of HeLa cells transfected with control (siCTRL) or MMS22L (siMMS22L) siRNAs. Arrows indicate direction of DNA synthesis. Green, CldU; red, IdU; blue, DNA. Scale bar: 50 kb.

(B) Box plot representation of IdU tract lengths in cells transfected with control and MMS22L siRNAs. The number within each box indicates the median of the result. Each box plot consists of data from three independent experiments and represents a total of 160 measurements. *p*-values between the indicated samples were calculated using a non-parametric Mann-Whitney test.

(C) Fork velocities derived from the experiment depicted in A-B. Data are represented as the mean ± SD.

(D) Above is a schematic of the CPT recovery experiment. Below are representative images of single DNA fibers from the fork recovery experiment. Arrows indicate direction of DNA synthesis. Colors are as in (A).

(E) Box plot representation of IdU tract lengths in cells transfected with control and MMS22L siRNAs. The number within each box indicates the median result. Each box plot consists of data from 2 independent experiments and represents a total of 200 measurements. *p*-values were calculated as in (B).

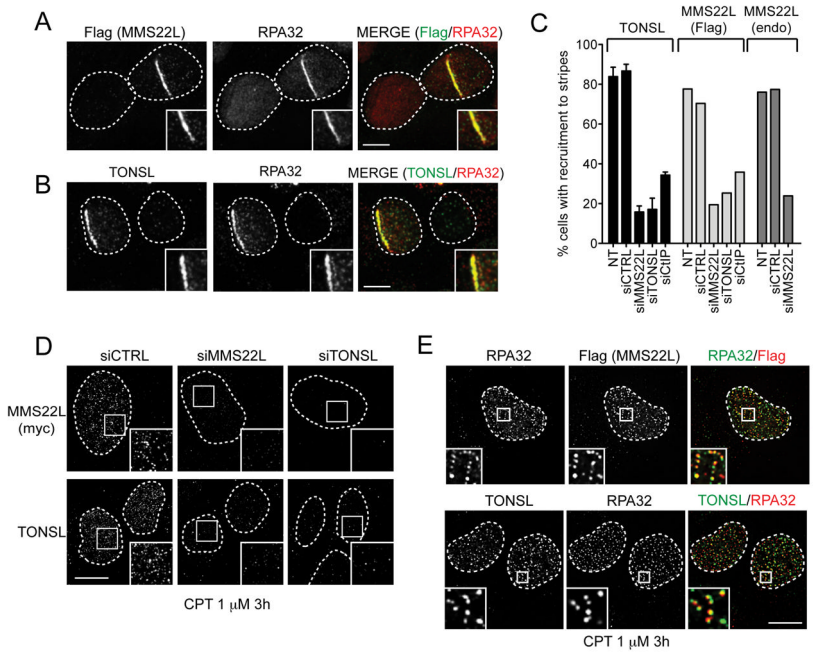

Figure 5. MMS22L and TONSL accumulate at sites of DNA damage

(A-B) U2OS cells expressing MMS22L-mFlag (A) or unaltered U2OS cells (B) were microirradiated with a UVA laser and processed for RPA32 and Flag (MMS22L; A) or TONSL

(B) immunofluorescence. Dashed lines indicate nuclei as determined by DAPI staining (not shown). Scale bar: 10 μm.

(C) Quantitation of the percentage of cells with a γ-H2AX stripe that also contained a MMS22L or TONSL stripe after transfection with the indicated siRNAs. The experiments were done with U2OS cells stably expressing MMS22L-mFlag (for the Flag staining) or unaltered U2OS cells for the endogenous (endo) TONSL and MMS22L staining. At least 80 cells per condition were counted. See Figure S6A-C for representative micrographs.

(D) U2OS cells stably expressing MMS22L-mFLag (top) or unaltered U2OS cells (bottom) were transfected either with control (siCTRL), MMS22L (siMMS22L) or TONSL (siTONSL) siRNAs. 48 h after transfection, cells were treated with 1 μM CPT for 3 h before being fixed and processed for myc (MMS22L; top) or TONSL (bottom) immunofluorescence. Dashed lines indicate nuclei as in (A). Scale bar: 10 μm.

(E) U2OS cells stably expressing MMS22L-mFlag (top) or unaltered U2OS (bottom) were treated with 1 μM CPT for 3 h before being fixed and processed for RPA32 and Flag (MMS22L; top) or TONSL (bottom) immunofluorescence. Dashed lines indicate nuclei as in (A). Scale bar: 10 μm.

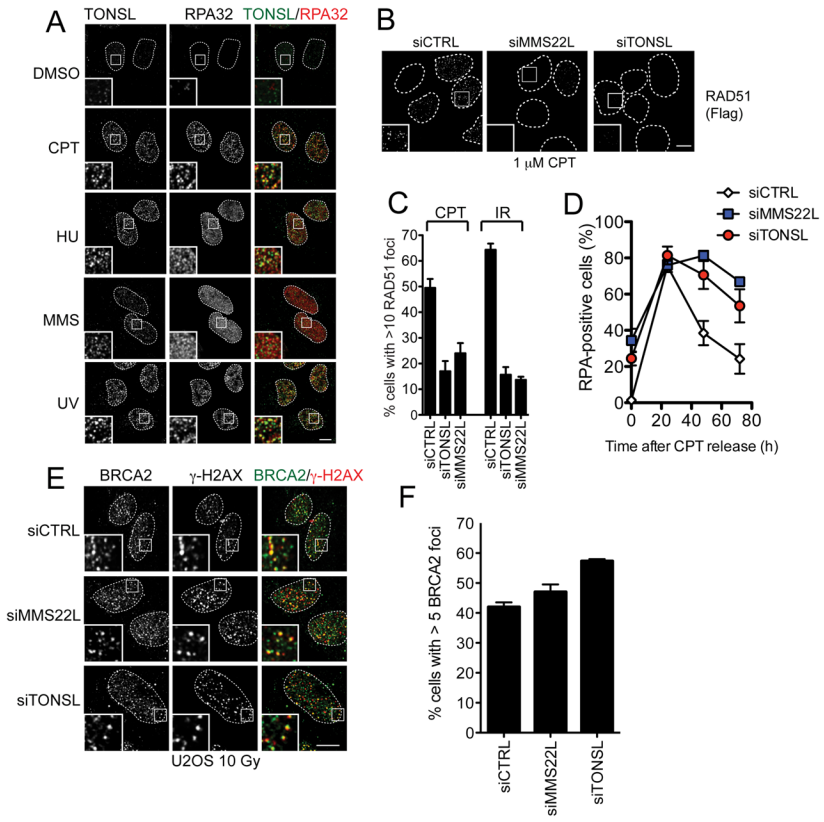

Figure 6. MMS22L and TONSL colocalize at stalled replication forks

(A) U2OS cells were treated with DMSO or the indicated DNA damaging agents (1 μM CPT for 3 h, 3mM HU for 2 h, 0.02% MMS for 2 h, 50 J/m^2 UV-irradiation followed by 2 h recovery). Cells were then fixed and processed for TONSL and RPA32 immunofluorescence. Dashed lines indicate nuclei as determined by DAPI staining (not shown). Scale bar: 10 μm.

(B) U2OS cells stably expressing Flag-tagged RAD51 were transfected either with control (siCTRL), TONSL (siTONSL) or MMS22L (siMMS22L) siRNAs. 48 h after transfection, cells were treated with 1 μM CPT for 3 h before being fixed and processed for Flag immunofluorescence. Dashed lines indicate nuclei as in (A). Scale bar: 10 μm.

(C) Quantitation of Flag-RAD51 foci from the experiment described in (A) and from an identical experiment done with 10 Gy ionizing radiation instead of CPT. Foci-positive cells were defined as cells with more than 10 Flag-RAD51 foci. At least 100 cells per condition were counted. Data are represented as the mean ± SD (n=3).

(D) Quantitation of RPA foci in U2OS cells treated with 0.5 μM CPT for 30 min (t=0) and then released from the treatment and collected at the indicated time points. Representative images are shown in Figure S7B.

(E) U2OS cells were transfected with control, MMS22L or TONSL siRNAs. 48 h after transfection, cells were irradiated with 10 Gy and 4 h later were fixed and processed for BRCA2 and γ-H2AX immunofluorescence. Insets are magnifications of the indicated fields. Dashed lines indicate nuclei as in (A). Scale bar: 10 μm.

(F) Quantitation of BRCA2 foci from the experiment described in (E). Foci-positive cells were defined as cells with more than 5 BRCA2 foci. At least 75 cells per condition were counted. Data are represented as the mean ± SD (n=3).

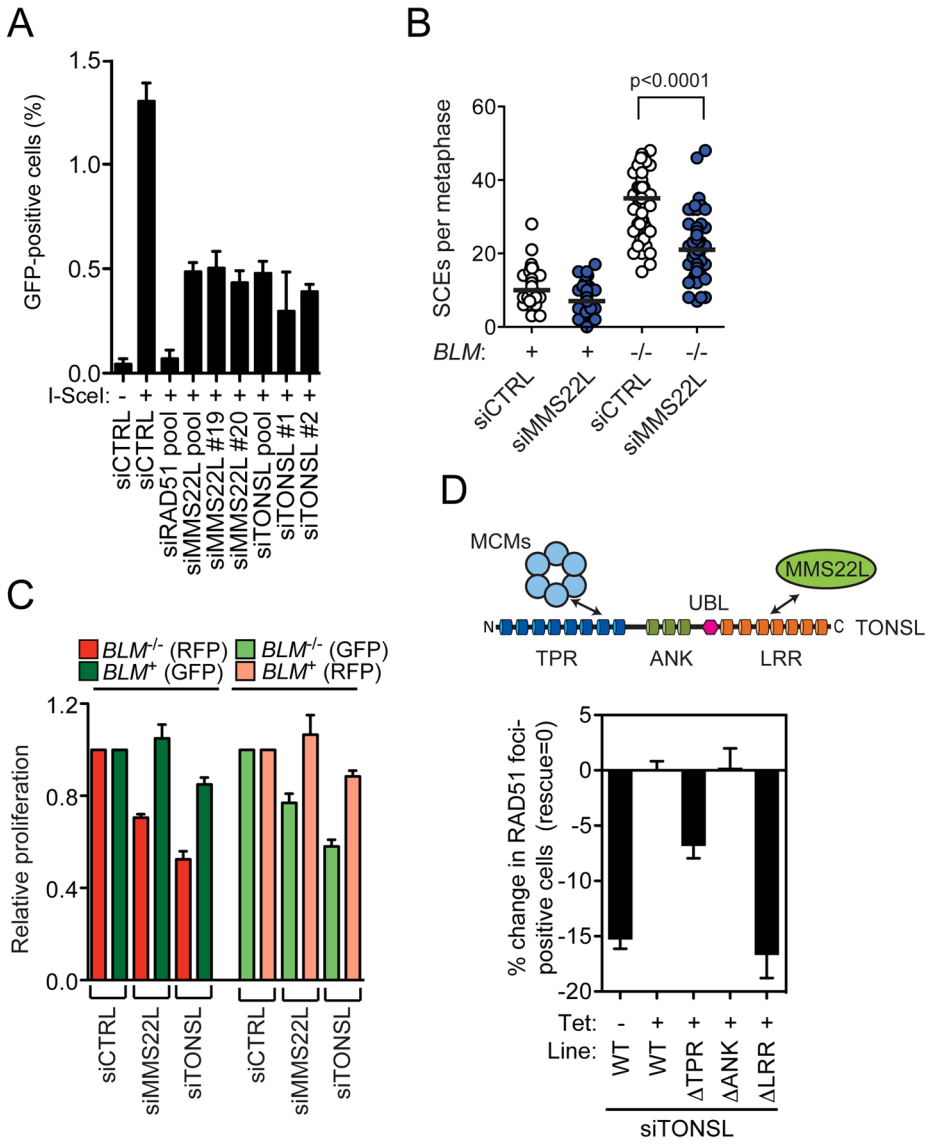

Figure 7. The MMS22L-TONSL complex promotes homologous recombination

(A) Effect of MMS22L or TONSL depletion on homologous recombination. HeLa DR-GFP cells were transfected with the indicated siRNAs, and 48 h later were transfected with or without an I-SceI expression plasmid. 48 h after transfection, cells were harvested and assayed for GFP expression by FACS analysis. Data are represented as the mean ± SD (n=3).

(B) Effect of MMS22L depletion on sister chromatid exchange in BLM deficient cells (PSNG13; *BLM*$^{-/-}$) and isogenic complemented cells expressing *BLM* cDNA (PSNF5; *BLM*$^{+}$) transfected with control (siCTRL) or MMS22L siRNAs. At least 40 metaphase cells were counted for each condition. Statistical significance was calculated with a Mann-Whitney test.

(C) Bloom syndrome cells (*BLM*$^{-/-}$) and isogenic complemented cells expressing *BLM* cDNA (*BLM*$^{+}$) were first transduced with a lentivirus expressing either GFP or RFP. The resulting fluorescent protein-marked *BLM*$^{-/-}$ and *BLM*$^{+}$ lines were plated at a 1:1 ratio and were transfected with control, MMS22L, or TONSL siRNAs. 96 h post-transfection cells were fixed and imaged with a high-content microscope to determine the *BLM*$^{-/-}$ to *BLM*$^{+}$

ratio. Data was normalized to the control siRNA condition to eliminate proliferation and transfection differences between cell lines. The data represents the mean +/− SEM (n=2). (D) The TONSL LRR and TPR repeats are required for RAD51 focus formation. Top: Schematic representation of the domain architecture and physical interactions of TONSL. U2OS cell lines containing stable integrations of the indicated TONSL cDNA were transfected with a TONSL siRNA (#1) and were either left uninduced (−) or were induced (+) by tetracycline (Tet) addition for 24 h prior to a 10 Gy IR dose. 3h later, the cells were fixed and processed for RAD51 immunofluorescence. The number of cells with more than 5 RAD51 foci is presented as the percentage deviation from the wild type, induced condition.